ELSEVIER

Surface Science 360 (1996) 180–186

surface science

Steps and facets on annealed $LaAlO_3\{100\}$ and $\{110\}$ surfaces

Z.L. Wang *

School of Materials Science and Engineering, Georgia Institute of Technology, Atlanta, GA 30332-0245, USA

Received 14 October 1995; accepted for publication 19 January 1996

Abstract

Lanthanum-aluminate ($LaAlO_3$) is one of the optimum substrates for epitaxic growth of thin oxide films. In this paper, the structures of the {100} and {110} surfaces of annealed $LaAlO_3$ are studied using reflection electron microscopy (REM). ⟨010⟩ steps have been observed on {100}, these are the lowest energy steps. The {100} surface is atomically flat, but the {110} surfaces exhibit high-density fine structures distributed on large surface terraces. These fine structures correspond to the formation of small width (100) and (010) facets on the (110) surface. A growth model is given to interpret the formation of large steps and large terraces on the {110} surfaces.

Keywords: Lanthanum aluminate; Reflection electron microscopy (REM); Reflection high-energy electron diffraction (RHEED); Stepped single crystal surfaces; Surface structure, morphology, roughness, and topography

1. Introduction

Lanthanum-aluminate ($LaAlO_3$) is an optimum substrate for epitaxic growth of high temperature superconductors, ferroelectric thin films and colossal magnetoresistive (CMR) magnetic oxides. Unfortunately, most of the oxide thin films have been grown on substrates without careful characterization and in some cases, the films were grown on as-received, polished substrates supplied commercially. This could be a serious problem which affects the quality and growth of the oxide films. In additional to the requirements of smallest lattice mismatch and structure match, it has been recently observed that the nucleation and growth of thin films are strongly affected by the structures, such as steps and dislocations, of the substrate surfaces. A direct correlation between the growth of columnar defects in $YBa_2Cu_3O_{7-x}$ and the steps on the $LaAlO_3$ substrates has been observed [1,2]. For $La_{1-x}Sr_xCoO_3$ CMR materials, the formation of {100} planar stacking faults is due to the presence of steps on the MgO substrate [3]. It is thus essential to examine the substrate surface to control the nucleation and improve the quality of thin films.

Most of the oxide films were grown using either metallic organic chemical vapor deposition (MOCVD) or laser ablation techniques under non-ultra high vacuum (non-UHV) condition. In general, the oxide surface is reasonably stable and shows less reactivity with the environmental. Therefore, it is possible to use surface analysis techniques which are performed under non-UHV conditions for studying the surfaces of oxides.

* Corresponding author. Fax: +1 404 8949140; e-mail: zhong.wang@mse.gatech.edu.

0039-6028/96/$15.00 Copyright © 1996 Elsevier Science B.V. All rights reserved
PII S0039-6028(96)00583-3

Reflection electron microscopy (REM) is a powerful technique for examining step structures on the surfaces of single crystalline materials [4–6]. In REM, the incident electrons strike the crystal surface at a glancing-angle of a few degrees. This is the geometry for reflection high-energy electron diffraction (RHEED). REM images were formed by selecting a reflected Bragg beam using the objective aperture in transmission electron microscopy (TEM). This dark-field imaging technique has high surface sensitivity and can be easily applied to image atomic steps on single crystal surfaces. REM has been previously applied to study the {100} surfaces of annealed $LaAlO_3$ [7,8]. [010] and [001] steps have been observed and the surface showed the 5×5 reconstruction.

In this paper, REM is applied to study the {110} surfaces of $LaAlO_3$. The {110} surface is found to be not atomically flat but composed of small {100} facets. The growth of large surface steps on {110} is observed and is interpreted using a {100} facet model. Experimental evidence which shows the 5×5 reconstruction of the {100} facets on the {110} surface is also illustrated. For the convenience of data analysis for {110}, the step structures on the {100} surfaces are outlined in Section 2.1. Detailed experimental results and analysis of the {110} surface will be given in Section 2.2.

2. Experimental results and analysis

REM experiments were performed using a Philips 400 (120 kV) TEM under a vacuum of 10^{-6} to 10^{-7} Torr. Bulk specimens were prepared by cutting $LaAlO_3$ single crystal sheets into samples with dimensions of about $2.5 \times 1 \times 0.8$ mm. The {100} and {110} surfaces were mechanically polished before annealing. The polished samples were annealed at 1500°C for 10 or 20 h in air. Detailed experimental method and contrast mechanism of REM are given elsewhere [5].

The crystallographic data on $LaAlO_3$ have been given by Geller and Bala [9] and Berkstresser et al. [10]. The structure is the distorted-perovskite structure with lattice constants $a=b=c=$ 0.3788 nm and $\alpha=\beta=\gamma=90.066°$. The structure is referred to as a face-centered rhombohedral cell, in which the La^{+3} ion locates at (000), the Al^{+3} ion at (0.5 0.5 0.5), and the O^{-2} ions at the face-centers {0.5 0.5 0}. {100} twins are present in $LaAlO_3$ due to the distorted-perovskite structure.

2.1. $LaAlO_3$ {100}

For the convenience of interpreting the structure of $LaAlO_3$ {110}, in this section. the surface structure of $LaAlO_3$(100) determined by REM is summarized. Fig. 1 shows a [001] RHEED pattern of the annealed $LaAlO_3$ (100) surface. In additional to the strong Bragg reflections of the bulk $LaAlO_3$, two strong superstructure reflections are observed between bulk reflections (10 0 0) and (10 $\bar{1}$ 0). The two superstructure reflections are separated by 1/5(0$\bar{2}$0) and 1/5(020), respectively, from the (10 0 0) and (10 $\bar{1}$ 0) bulk reflections. On the right-hand side of the (10 $\bar{1}$ 0) reflection, four equally-spaced superstructure reflections are seen, as indicated by arrowheads. These superstructure reflections correspond to the formation of a 5×5 reconstruction on the surface, as observed previously by high-resolution REM imaging [8]. The splitting of the superstructure reflections is due to the {100} twins present in bulk $LaAlO_3$, and the twin angle is as small as 0.13° [7].

On the {100} surface, the most striking phenomenon is the faceted <100> steps. Fig. 2a is a REM image recorded with the (10 0 0) specularly reflected beam under the diffracting condition shown in Fig. 1, in which the azimuth of the

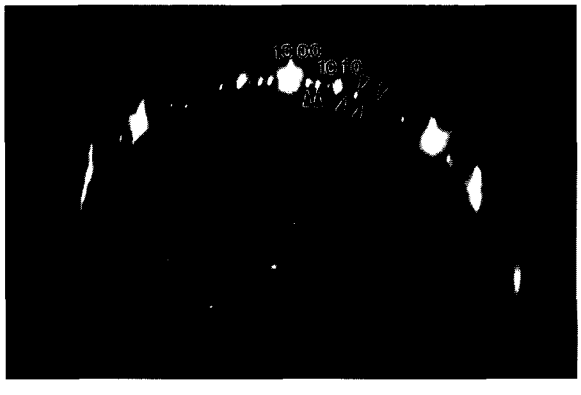

Fig. 1. [001] RHEED pattern from an annealed $LaAlO_3$(100) surface showing a 5×5 surface reconstruction.

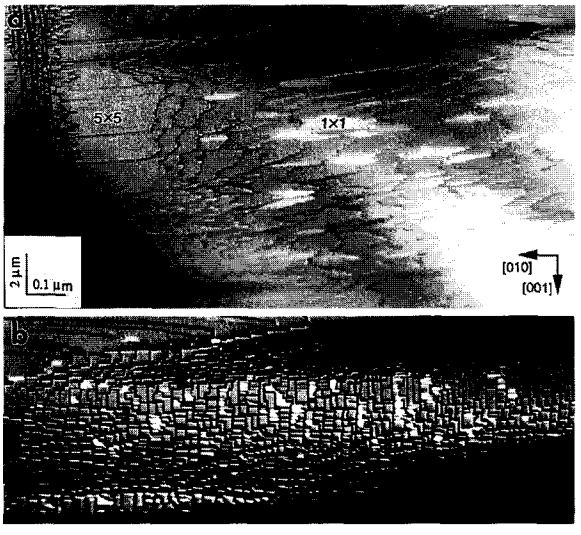

Fig. 2. REM images of the $LaAlO_3$ (100) surface showing the [010] and [001] steps. The images were recorded using the (10 0 0) specularly reflected beam under the diffracting condition shown in Fig. 1. Beam azimuth is [001].

incident beam is exactly parallel to the [001] zone-axis. In the REM image, the 5×5 reconstructed area shows darker contrast due to the reduction of the (10 0 0) reflected beam intensity as the result of exciting the superstructure reflections, which are not included in the angular selection range of the objective aperture of the TEM. The unreconstructed surface areas show brighter contrast. The [010] and [001] steps are observed over the entire image. The regions which show brighter and darker contrast sometime share the same terrace, and there is no step between them. Fig. 2b shows an REM image of a surface region with a small miscut with respect to the exact crystallographic (100) plane. Many [010] and [001] steps are seen. The larger steps are about 2–3 unit cells in height [7]. The areas showing darker contrast exhibit a 5×5 reconstruction and the unreconstructed areas show brighter contrast. In general, the entire surface is almost completely covered by the reconstructed layer.

When the specimen was annealed at 1500°C, the high mobility and long range diffusion of the surface atoms tends to reconstruct the surface morphology. The surface atoms moved to the positions where they have the lowest energy. The REM observations show that the ⟨100⟩ steps preserve the lowest energy in comparison to steps along any other direction on the {100} surfaces. Also, the {100} facets have the lowest energy, resulting in the observed faceted structures. It must be pointed out that the ⟨100⟩ faceted steps have limited length so that a long step can be composed of [001] and [010] stair-type segments. These conclusions will be used in the next section to interpret the structure of the {110} surfaces.

2.2. $LaAlO_3\{110\}$

In this section, the REM and RHEED studies of $LaAlO_3\{110\}$ surfaces are reported. The {110} surfaces were prepared under the same conditions as for {100}. Fig. 3 shows an REM image of the {110} surface after being annealed at 1500°C for 10 h in air. An RHEED pattern under which the image was recorded is shown in Fig. 3b. In REM, the step configuration is least distorted if the azimuth of the incident beam is parallel to [001]. Unfortunately, for the (110) surface in particularly, the [001] zone axis diffraction gives a weakly reflected beam and the surface resonance condition is not satisfied (see Fig. 9a). It is only under the diffracting condition shown in Fig. 3b that a reasonable REM image could be obtained. The (110) surface exhibits the "roof-tile" structure, showing many terraces. The length of the terrace along [001], approximately the incident beam direction (from the top to the bottom of the image), is much larger than its width along $[1\bar{1}0]$ if the foreshortening effect is considered. The terrace is not

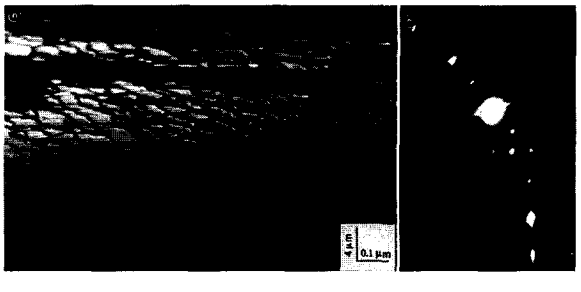

Fig. 3. (a) REM image of the $LaAlO_3$(110) surface, annealed at 1500°C for 10 h in air, showing the formation of surface terraces. (b) RHEED pattern used to record the image. Beam azimuth is near [001].

atomically flat but consists of many fine structures. The step height is of the order of 5 nm, much larger than the step height observed on {100}. The edges of the terraces are in curved shapes that are not parallel to any low index zone axis.

Although the entire surface exhibits the roof-tile structure, some surface areas show larger terraces, as illustrated by the REM image in Fig. 4. It is apparent that the steps separating the larger terraces are higher than those separating the smaller terraces. The smaller terraces are the dominant structure at this stage. The population of the larger terraces increases significantly with the increase of annealing time. Fig. 5 shows an REM image of the {110} surface after annealing at 1500°C for 20 h. The widths of surface terraces have increased by a factor of approximately three in comparison to those shown in Fig. 4. The heights of steps between terraces are also increased by the same magnitude. Again many fine step-like structures remain on each terrace, as seen in the enlarged area shown in the inset. The density of the fine steps is so high that each individual step cannot be resolved in the REM image due to the foreshortening effect. The foreshortening effect can also strongly influence the orientation of the steps in a real REM image, making it difficult to directly identify the step direction unless the azimuth of the incident beam is exactly parallel to the zone axis, such as [001].

Fig. 4. REM image of the $LaAlO_3$(110) surface, annealed at 1500°C for 10 h, showing the coexistence of large and small terraces on the surface. The image was recorded under the diffracting condition shown in Fig. 3b.

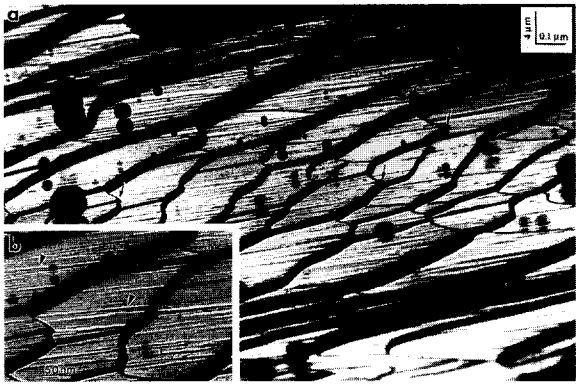

Fig. 5. (a) REM image of the $LaAlO_3$(110) surface, annealed at 1500°C for 20 h, showing the increase in the population of large surface terraces in comparison to those shown in Fig. 3. The arrowheads indicate possible {100} facets. (b) Enlargement of the image showing fine step-like contrast on surface terraces. Beam azimuth is near [001]. The image was recorded under the diffracting condition shown in Fig. 3b.

However, the diffracting condition, as to be shown in Fig. 9a, does not produce a strong surface resonance effect and the reflected intensity of the specular beam is rather weak, resulting in poor image contrast which does not allow the separation of surface steps of a few nanometers in width. The (110) surface does not exhibit the atomic flatness as the {100} surface does. It is apparent that the sizes of surface terraces increase dramatically with increasing annealing time. The surface morphology exhibits an entirely different image in comparison to that of {100}.

The images shown in Figs. 3–5 were recorded under the diffracting condition shown in Fig. 3b. In this case, the deviation angle of the incident beam direction from the [001] zone axis is approximately 80 mrad, which is about twice as large as the incident angle of the beam. Therefore, the distortion of the image is quite severe, particularly when the surface steps are not straight.

To image the facets on the (110), a simple technique illustrated below is used. The incident beam is deflected and the specimen is tilted to satisfy a diffracting condition under which one of the beams, that is propagating exactly parallel to the (110) crystallographic plane (i.e., the surface terraces), is used for recording the REM image. This beam is mainly contributed by the electrons

which are propagating parallel or nearly parallel to the surface due to the resonance effect (see the strong beam near the surface in Fig. 3b). Fig. 6 shows an REM image recorded using the Bragg beam indicated with an arrowhead, the exit angle of which is approximately 3 mrad. The imaging of this beam directly light up the step edges, since the electrons are traveling parallel to the (110) crystallographic plane, and the step height is simply the distance between two adjacent bright lines in the image. The step height measured from this image does not suffer any foreshortening effect. The step height is approximately 20 nm. More importantly, the step edges do not show a straight line but a smooth "saw-teeth" type contrast, indicating the presence of facets on the (110) surfaces. The average distance between the observed facets is approximately 70 nm. The angle between the facets would be 90° if the adjacent facets were large planar (100) and (010). In contrast, the angle measured from the image is approximately 160°. This angle is possible only if the observed saw-teeth large facets are composed of small stair-like (100), (010) and (001) facets at nanometer scale. In the images shown in Figs. 3–5, the foreshortening along the beam direction makes these fine facets hardly resolvable.

From the studies of the {100} surface, we have found that the ⟨100⟩ steps and {100} facets have the lowest energy. This result can be applied to interpret the morphological structural evolution of the {110} surfaces during annealing. Starting from the beginning of specimen preparation, an as-polished surface is rough consisting of many hills and valleys. A small miscut is present between the surface and the {110} crystallographic plane. Surface diffusion starts when the sample is annealed, leading to the formation of small terraces, which are believed to have lower surface energy than a rough surface. REM images shown in Figs. 3–5 indicate that there are many fine structures (or steps) on the (110) terraces, which may correspond to the formation of small width (100) and (010) facets on the surface, as schematically shown in Fig. 7a for a case in which the facet edges are assumed to be parallel to the terrace. The (100), (010) and (001) facets are favored due to low energy, and these facets remain on the surface even when the surface is annealed for an extensive period of time. The assembling configurations made by these fine facets can create various

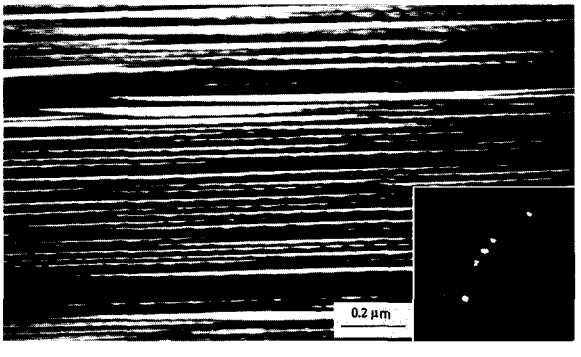

Fig. 6. REM image of the $LaAlO_3$(110) surface recorded using a reflected beam, as indicated by an arrowhead in the inset RHEED pattern, which is propagating parallel to the (110) crystallographic plane. The oscillation of the step edges indicate faceting on the surface. Beam azimuth is near [001].

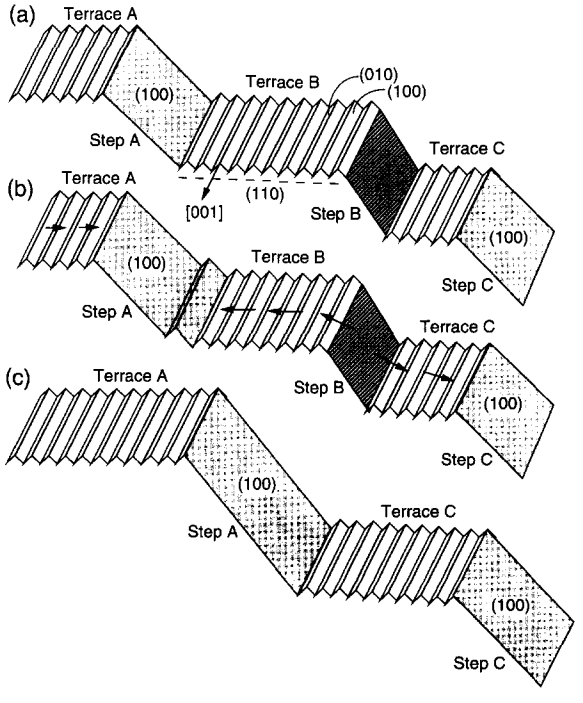

Fig. 7. Schematic showing the evolution of the surface morphology of $LaAlO_3$(110), formed by many small width (100) and (010) facets, during annealing. The width of the small facets is in nanometer scale. Steps between (110) terraces possibly correspond to (100) surfaces and other high index planes.

surface geometries. In addition to the (100) and (010) facets shown in Fig. 7, (001) facets can also exist on a (110) surface. For simplicity, the (100) and (010) facets are assumed as the basic components for the following discussion.

The large terrace steps could also be (100) facets. These faces grow when atoms diffuse from the inner steps (on the (110) terrace) towards the edge of the terrace, as indicated by arrowheads in Fig. 7b, resulting in the growth of step height for a step A. For a high index step, such as a step B in Fig. 7a, the atoms tend to diffuse towards steps A and C, (100) faces having the lowest surface energy, resulting in the reduction in height and width of terrace B and the increase in heights and widths of terraces A and C. This process continues until terrace B disappears, as shown in Fig. 7c. Thus, the sizes and heights of terraces A and C are increased. This is consistent with the experimental observations shown in Figs. 3–5.

There are two ideal models for forming {100} facets on the (110) surface, as schematically shown in Fig. 8. For a (110) surface without miscut, (100) and (010) facets can form a 90° saw-teeth structure (Fig. 8a). These facets are parallel to the incident beam direction [001]. If the sizes and heights of these facets are adjusted, a non-even surface morphology, as shown in Fig. 8b, can be produced. The angle between the dashed lines represents the angle between the two large "facets", which is 160° as for the case shown in Fig. 6. For a (110) surface with a small angle of miscut, the (001) and (110) facets are expected to form (Fig. 8c). If the crystal surface was composed of one type of the structure, such as the one shown in Fig. 8a, straight steps would be observed in REM images. However, the REM images shown in Figs. 4 and 5 indicate that the surface steps at relatively lower resolution and image magnification are curved. Therefore, the surface steps are believed to be composed of small-size segments composed of facets combining both models shown in Figs 8a and 8c, resulting in complex curved steps that may be parallel to neither [001] or [1$\bar{1}$0]. The changes in lengths and widths of those segments can make large scale curved surface steps along various directions. The growth of (100), (010) and (001) according to Fig. 7 can produce various surface geometries. Unfortunately, the foreshortening effect makes it difficult to resolve the densely distributed features separated by a few nanometers.

From the RHEED and REM results on the {100} surface, the 5×5 reconstruction is always seen on the surface. Thus, the {100} facets on the {110} surface may also exhibit the same type of reconstruction. To find possible evidence related to this reconstruction, RHEED patterns were recorded from the {110} surface, as shown in Fig. 9. Some faint superstructure reflections due to surface reconstruction are seen, as indicated by arrowheads in Fig. 9a. The superstructure reflections are easiest to be seen along the direction

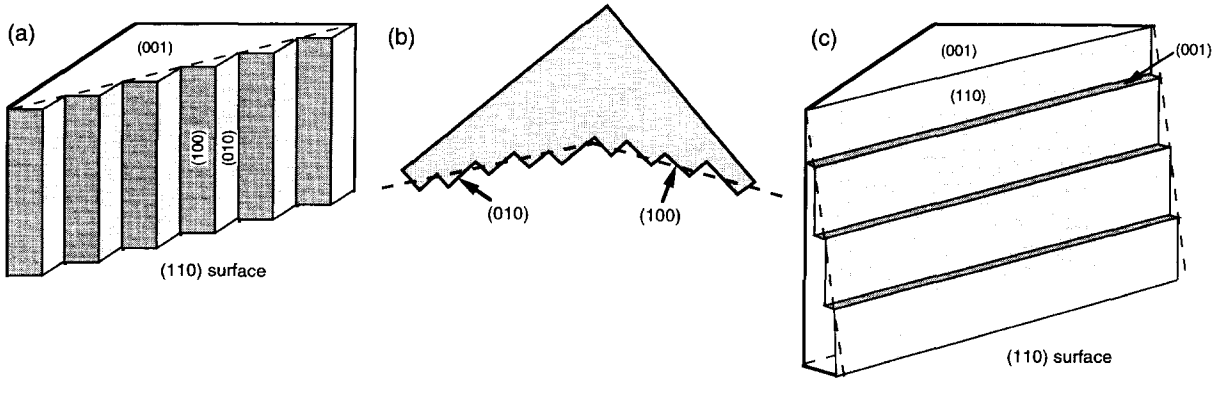

Fig. 8. (a), (c) Two ideal models for the formation of {100} facets on the (110) surface. (b) Surface profile if the sizes and the heights of the (100) and (010) facets are adjusted.

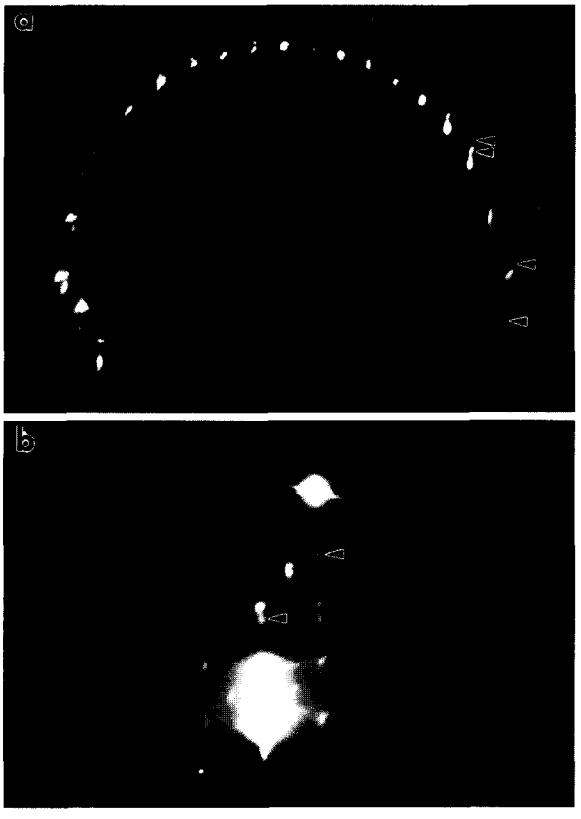

Fig. 9. RHEED patterns recorded from the (110) surface when the incident beam is nearly parallel to [001] showing some superstructure reflections which are possibly generated by the reconstruction of the {100} facets on the surface.

perpendicular to the surface, particularly near the edge of the crystal, because of the diffracting condition as described by the Ewald sphere construction. The absence of superstructure reflections along the direction perpendicular to the beam and parallel to the surface is probably due to the intersecting geometry of the Ewald sphere with the reciprocal lattice spots. In Fig. 9b, some of the superstructure reflections are apparent, but the angle between these beams could vary because of the severe refraction effect particularly when the Bragg angles are small [11].

3. Conclusions

In this paper, the {100} and {110} surfaces of $LaAlO_3$ have been studied by RHEED and REM. Numerous [010] and [001] surface steps are observed on the {100} surfaces of $LaAlO_3$. The ⟨100⟩ steps preserve the lowest energy in comparison to steps along other directions on {100}. The terraces on the {100} are atomically flat. Most of the {100} surface areas are covered by the 5×5 reconstructed layer.

$LaAlO_3${110} exhibits numerous high-step terraces, and each terrace shows fine-step contrast. The size of terraces and the height of the steps increase with increasing annealing time, but the fine step-like structure remains throughout. The fine structures observed on {110} terraces are interpreted as due to the formation of small-width {100} facets. This model can interpret the structural evolution observed on the {110} surfaces, and experimental results seem to support this model.

References

[1] Z.L. Wang, D.H. Lowndes, D.K. Christen, D.M. Kroeger, C.E. Klabunde and D.P. Norton, Physica C 252 (1995) 125.
[2] D.H. Lowndes, D.K. Christen, C.E. Klabunde, Z.L. Wang, D.M. Kroeger, J.D. Budai, S. Zhu and D.P. Norton, Phys. Rev. Lett. 74 (1995) 2355.
[3] Z.L. Wang and J. Zhang, Philos. Mag. A 72 (1995) 1513.
[4] J.M. Cowley, Prog. Surf. Sci. 21 (1986) 209; Z.L. Wang, Rep. Prog. Phys. 56 (1993) 997.
[5] Z.L. Wang, Reflection Electron Microscopy and Spectroscopy for Surface Analysis (Cambridge University Press, 1996).
[6] K. Yagi, Surf. Sci. Rep. 17 (1993) 305.
[7] Z.L. Wang and A.J. Shapiro, Surf. Sci. 328 (1995) 141.
[8] Z.L. Wang and A.J. Shapiro, Surf. Sci. 328 (1995) 159.
[9] S. Geller and V.B. Bala, Acta Cryst. 9 (1956) 1019.
[10] G.W. Berkstresser, A.J. Valentino and C.D. Brandle, J. Cryst. Growth 109 (1991) 467.
[11] L.M. Peng and J.M. Cowley, J. Electron Microsc. Techn. 6 (1987) 43.